

# Mechanical Trapping of DNA in a Double-Nanopore System

*Sergii Pud<sup>1</sup>, Shu-Han Chao<sup>2</sup>, Maxim Belkin<sup>2</sup>, Daniel Verschueren<sup>1</sup>, Teun Huijben<sup>1</sup>, Casper van Engelenburg<sup>1</sup>, Cees Dekker<sup>1</sup> and Aleksei Aksimentiev<sup>2</sup>*

<sup>1</sup> Department of Bionanoscience, Kavli Institute of Nanoscience, Delft University of Technology, Van der Maasweg 9, 2629HZ Delft, Netherlands

<sup>2</sup> Department of Physics, University of Illinois at Urbana—Champaign, Urbana, Illinois 61801, United States

*\*The correspondence should be addressed to [c.dekker@tudelft.nl](mailto:c.dekker@tudelft.nl) or [aksiment@illinois.edu](mailto:aksiment@illinois.edu)*

## Contents

1. Additional examples of double-nanopore events.....	2
2. Characteristics of the end signatures of double-nanopore events.....	4
3. Coarse-grained MD simulations .....	5
4. TEM image of the asymmetric double-nanopore sample.....	8
5. Current blockade histograms recorded using an asymmetric double-nanopore system.....	9
6. Current blockade estimation using the model of Carlsen et al. <sup>5</sup> .....	10
7. Theoretical model of a blockade current .....	12
7.1 Verification of the theoretical model.....	15
7.2 Calculation of the conductance blockade for obliquely oriented DNA in a nanopore .....	16
8. Criteria for determining escape direction in a double-nanopore event.....	19
9. Additional set of experiments characterizing the entrance and exit of DNA from an asymmetric double-nanopore system. ....	20
10. Equivalent circuit for the asymmetric double-nanopore system.....	21
11. Calculation of the forces acting on the DNA in the access region .....	22
12. Movies generated by MD simulations.....	24

## 1. Additional examples of double-nanopore events

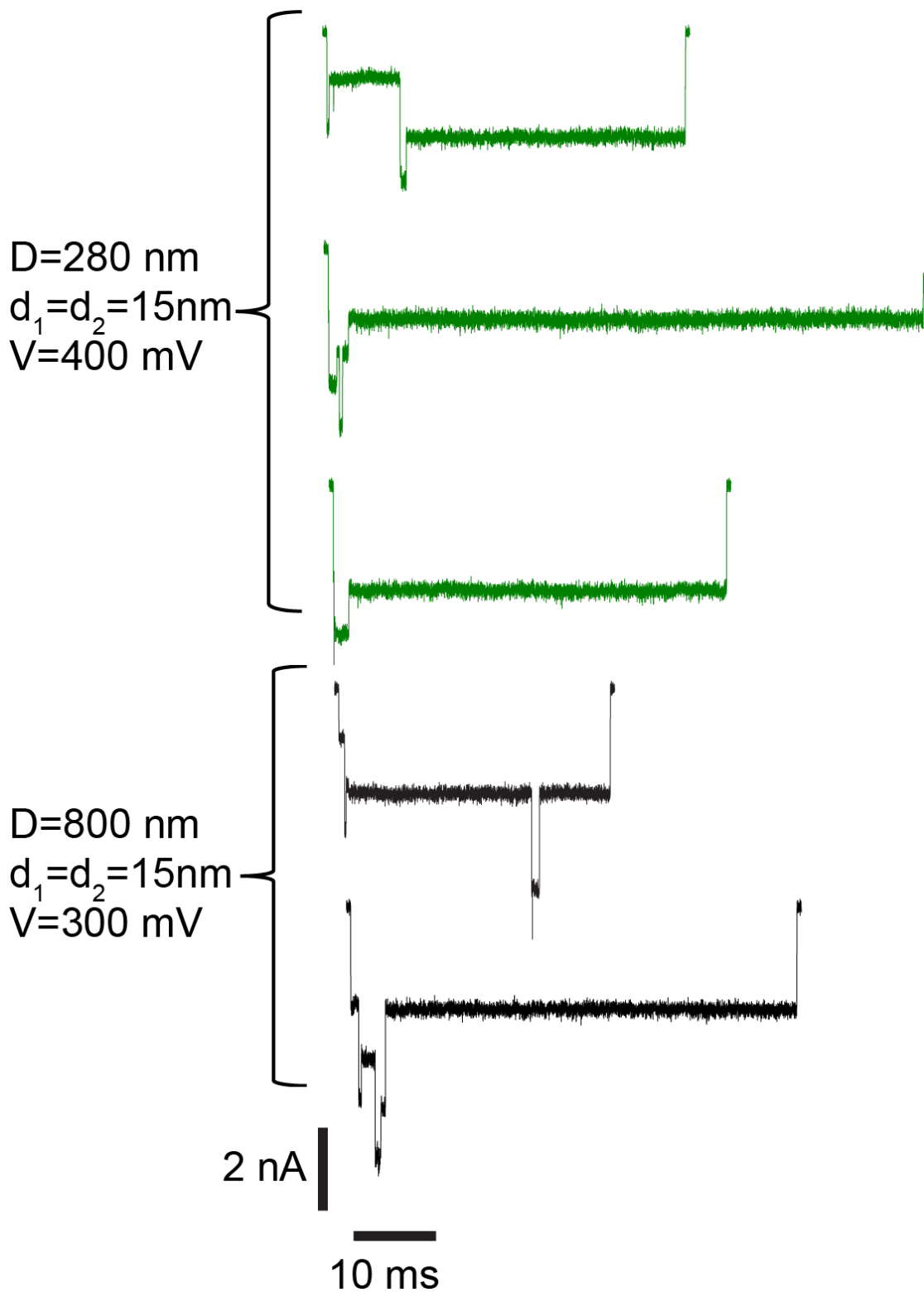


Figure S1. Examples of double-nanopore trapped events recorded using a system of two 15 nm-diameter nanopores separated by 280 (top) and 800 (bottom) nm.

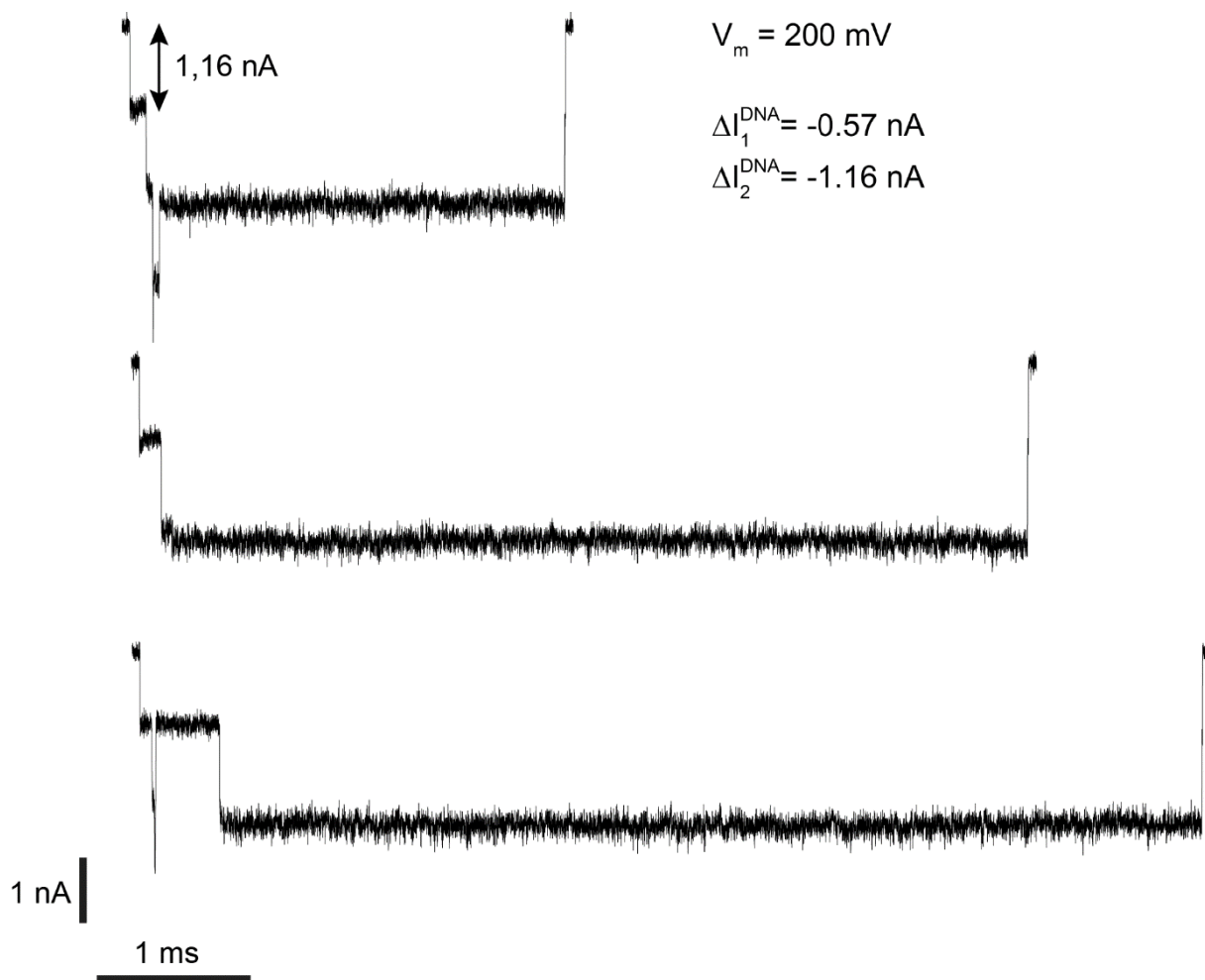


Figure S2. Examples of double-nanopore trapped events recorded using circular  $\lambda$ -DNA in a system of two 15 nm-diameter nanopores separated by 280 nm. The maximum extension of the circular DNA molecule (8  $\mu\text{m}$ ) is half that of its linearized variant. The ionic current blockades produced by circular DNA in individual nanopores double those produced by linearized (unfolded) DNA. The double-nanopore trapped event current level using circular DNA thus is four times the blockade level produced a single dsDNA strand in one nanopore.

## 2. Characteristics of the end signatures of double-nanopore events

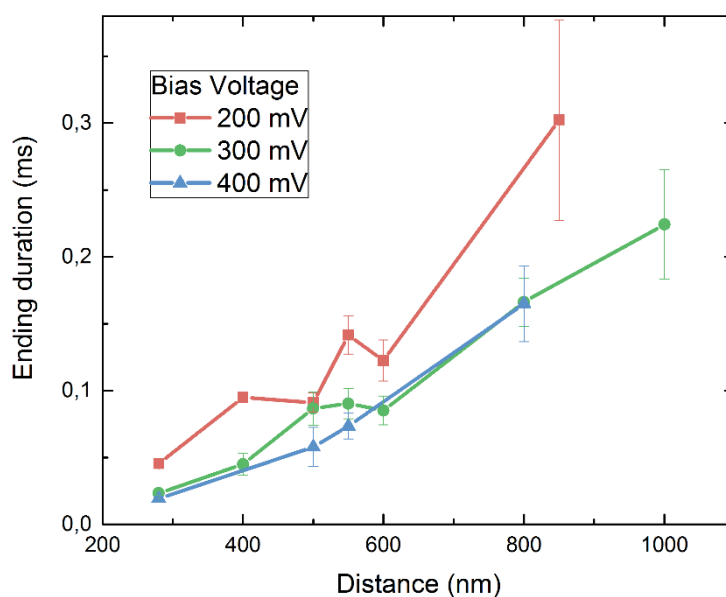


Figure S3. Duration of the ending signature of double-nanopore events (i.e., the brief single-blockade-level right before the final escape) as a function of distance between nanopores in a double-nanopore system. The end-signature duration increases with increasing pore-to-pore distance, as the latter increases the length that the lagging end of the DNA molecule has to traverse before exit.

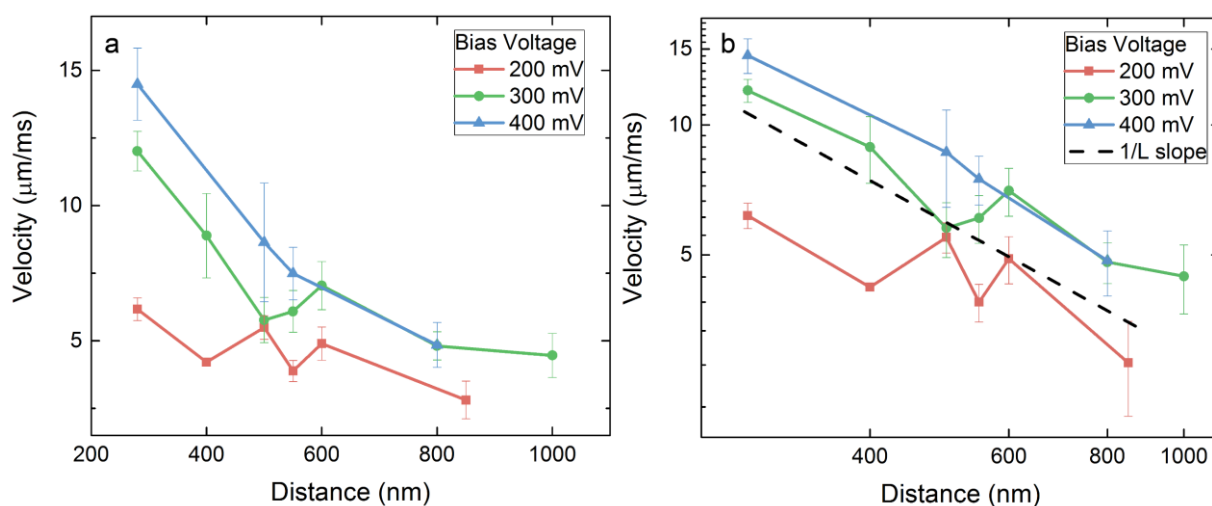


Figure S4. End velocity calculated using the end signature of the double-nanopore events, shown in normal scale (a) and in double-logarithmic scale (b). Black dashed line in (b) indicates a  $1/L$  slope. The  $1/L$  dependence of the escape velocity on distance suggests non-specific interactions between the DNA and the membrane surface where the friction force increases linearly with DNA-surface interaction length.

### 3. Coarse-grained MD simulations

The coarse-grained MD simulations were performed using a custom version of NAMD2<sup>1,2</sup>. Each ensemble simulation contained 2000 replicas in the double-nanopore trapping study and 200 replicas in the translocation control study. Each simulation system contained a 150-nucleotide ssDNA molecule described using our two-beads-per-nucleotide coarse-grained model<sup>2</sup> and a grid potential representing the steric interaction between DNA and the membrane. Given that the ratio of the persistence lengths of dsDNA and ssDNA is approximately 50, the 150 nucleotide fragment of ssDNA employed in our CG MD simulations corresponds to a ~4500 base pair fragment of dsDNA, a molecule ten times shorter than the one employed in our experiments. The steric potential was defined to have values of 0 and 5.85 kcal/mol assigned to the region of space occupied by the solution and the membrane, respectively. The grid spacing was 1 Å in each dimension. The membrane was 1 nm thick and each nanopore was 2 nm in diameter. The distance between the centers of the two pores was 5, 10 or 15 nm in the double-pore trapping study and 15 nm in the translocation control study. The distances reported in the main text reflect the 50-fold scaled up values, deduced by the 50:1 ratio of dsDNA/ssDNA persistence lengths. The simulation unit cell was a cube 105 nm on each side. Periodic boundary conditions and a nominal time step of 20 fs were employed. The tabulated nonbonded interactions were computed using a 34–35 Å cutoff. Stochastic forces from the solvent were introduced via a Langevin thermostat set to a temperature of 295 K and a nominal damping coefficient of 1.24 ps<sup>-1</sup>. The trajectories were recorded every 10,000 simulation steps. The time scale of the coarse-grained simulations was calibrated by matching the simulated electrophoretic mobility of a 150-nt CG ssDNA ( $5.8 \cdot 10^{-4} \text{ cm}^2 / (\text{V s}) = 6.44 L_{ss}^2 / (\text{V ns})$ , where  $L_{ss}$  is the persistence length of ssDNA) and the experimental free-draining mobility of dsDNA ( $4.2 \cdot 10^{-4} \text{ cm}^2 / (\text{V s}) = 1.58 \cdot 10^{-2} L_{ds}^2 / (\text{V ns})$ , where  $L_{ds}$  is the persistence length of dsDNA)<sup>3</sup>, yielding a 1 to 408 conversion factor between the ssDNA and dsDNA time scales. The time intervals reported in the main text already reflect the time scale calibration.

To set up initial conditions for DNA trapping simulations, one end of the DNA molecule was threaded through one of the nanopores. The terminal bead of the threaded end was restrained to remain at the center of the trans side exit of the nanopore. 2000 copies of the system were equilibrated for 300,000,000 simulation steps each (2.4 ms scaled time), producing 2000 random conformations of the polymer. During the equilibration, the terminal three beads

threaded through one of the two nanopores were subject to a cap grid potential (defined to have values of 11.7 kcal/mol at the cis region and 0 kcal/mol at the trans region and inside the nanopore) that prevented that end of the DNA molecule from escaping the nanopore; a 10 pN force pointing toward +z direction (the cis region) was applied to any bead of the DNA molecule that entered the volume of the other pore, preventing accidental double-nanopore trapping.

The double-nanopore trapping simulations were carried out starting from 2000 random conformations of DNA each having one end of the DNA threaded through one nanopore. The simulations were carried out in the presence of a grid potential that represented the effect of the transmembrane bias. Such transmembrane bias potentials were computed using the COMSOL Multiphysics program (version 4.4) for the double-nanopore geometry over a 2 Å-spaced grid; the details of the procedures are described in our previous study<sup>4</sup>. Subject to a transmembrane bias potential, each backbone bead of coarse-grained DNA experienced an electric force equal to the product of the local electric field and  $0.25 q^*$ , where  $q^*$  is the nominal charge of a DNA nucleotide. To prevent the end of the DNA initially threaded through the nanopore from escaping, the terminal three beads at the threaded end were subjected to a cap grid potential defined to have values 11.7 and 0 kcal/mol at the cis region and inside the nanopore, respectively. The size of the cap grid was  $7 \times 7 \times 0.3 \text{ nm}^3$ . The cap potential was applied only for the first 10,000,000 steps (80  $\mu\text{s}$  scaled time) of each DNA capture simulation. The forces on the beads produced by the steric, transmembrane bias and cap potential grids were calculated using the grid forces feature<sup>5</sup> of NAMD2. Each simulation was run until the DNA fully translocated from cis to trans side of the membrane.

For the study of force-differential control over DNA escape from a double-nanopore trap, both ends of the DNA molecule were initially threaded through both pores, one of each. One backbone bead was restrained to the center of each pore such that the lengths of the DNA fragments extending to the trans compartment from each pore were equal. The length of the middle portion, i.e. the segment exposed to the cis compartment, was chosen to approximately match the expected extension of the molecule<sup>2</sup> at the target force on the DNA in the nanopores. The actual tension in the DNA fragment at the cis side of the nanopore computed from the displacement of the restrained beads was  $4.1 \pm 1.1$ ,  $8.4 \pm 1.1$  pN and  $17.0 \pm 1.2$  for the 5, 10 and 20 pN target force, respectively. The systems were equilibrated for 50,000,000 steps (400  $\mu\text{s}$  scaled time), producing 200 random conformations for each target force. The translocation control simulations were carried out applying a constant external

force to each backbone bead of DNA confined within the nanopore volume via a custom tcl script. The total force on the beads in one of the nanopores was set to either 5, 10 or 20 pN, whereas the total force on all beads in the other pore was either equal to or 0.5, 1 or 2 pN less than the force in the first pore. Each simulation was run until the DNA fully translocated from cis to trans side of the membrane.

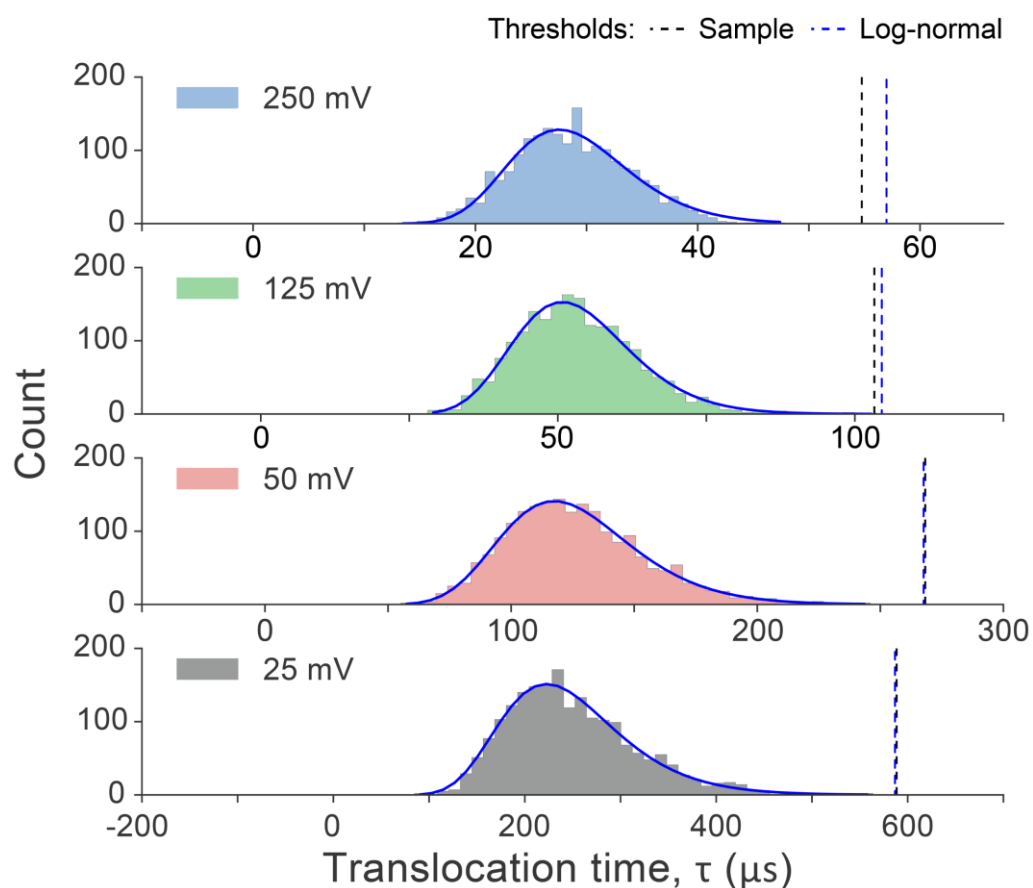


Figure S5. Distribution of single-pore DNA translocation times. The data shown are the same as in the main text Figure 4d, but now plotted on a linear time scale. Each histogram contains 40 bins. Blue solid lines show the log-normal fit (i.e. a Gaussian on a log scale) to each of the histograms. The thresholds, shown as dashed lines, were defined as the sample mean plus 5-fold sample standard deviation (black, same as in main text Figure 4d) or log-normal distribution mean plus 5-fold distribution standard deviation (blue).

#### 4. TEM image of the asymmetric double-nanopore sample

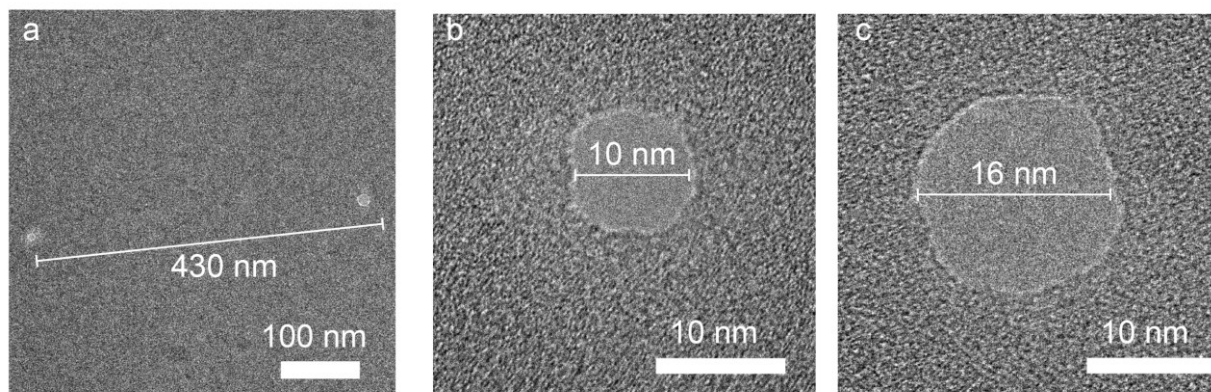


Figure S6. TEM image of an asymmetric double-nanopore system. (a) The distance between nanopores is 430 nm. The pore diameters are (b) 10 and (c) 16 nm.

## 5. Current blockade histograms recorded using an asymmetric double-nanopore system

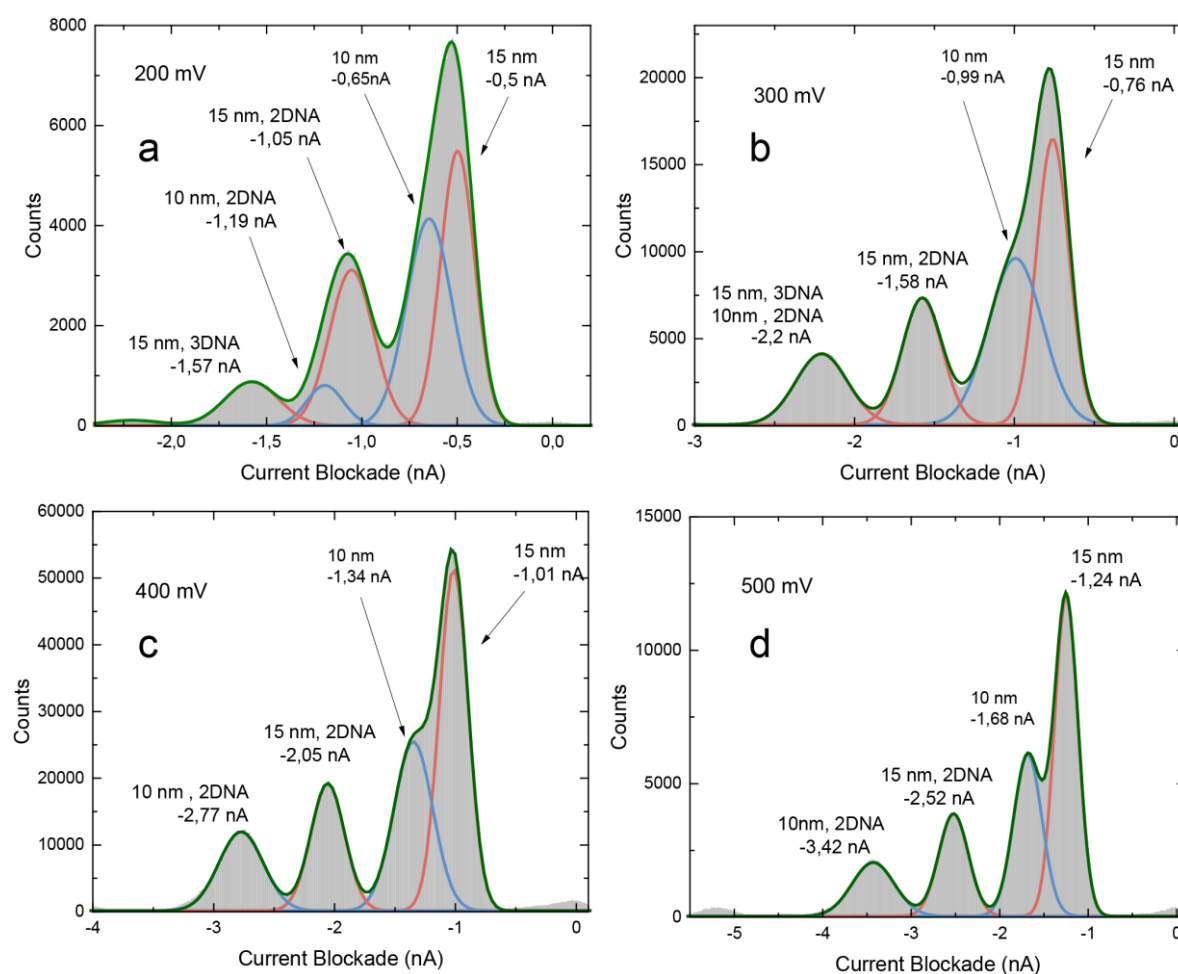


Figure S7. Histograms of experimental ionic current blockades produced by all DNA translocations through an asymmetric double-nanopore system and respective Gaussian fits. The diameters of the individual pores were 10 and 16 nm (see Fig. S6). Data in panels a, b, c, and d correspond to a transmembrane bias of 200, 300, 400 and 500 mV, respectively. The fitted peak values and the corresponding pore diameters are indicated on the graphs.

## 6. Current blockade estimation using the model of Carlsen et al. <sup>6</sup>

We estimated the current blockade values for single pore DNA translocations using the model published by Carlsen et al.<sup>6</sup>, where DNA is inserted in the middle of the nanopore. The conductance of each access region is

$$G_{acc} = 2\sigma d_p,$$

where  $d_p$  is the nanopore diameter and  $\sigma$  is the conductivity of the electrolyte, which in our case was taken as 13.2 S/m (measured value) for 2M LiCl solution. Taking into account the bulk and surface conductivity contributions, the conductivity of the pore region is defined as:

$$G_{pore} = \frac{\pi d_p^2}{4L_{eff}} \left( \sigma + \frac{4S\mu_{cation}}{d_p} \right)$$

where  $L_{eff}$  was taken as a fitting parameter close to  $L/3$  (see Ref. <sup>7,8</sup>). In our case of a 20 nm membrane it was taken as 5 nm,  $S$  is the surface charge density on SiN in LiCl solution, which was taken as<sup>9</sup> 0.03 C/cm<sup>2</sup>,  $\mu_{cation}$  is cation mobility of lithium, which was taken as  $4 \times 10^{-8} \frac{cm^2}{Vs}$ . The total nanopore conductance can be evaluated as<sup>8</sup>:

$$G_{Total} = \left( \frac{1}{G_{0pore}} + \frac{2}{G_{0acc}} \right)^{-1}$$

The DNA blocks the access region of nanopore and also occludes volume of the nanopore. We can calculate access and bulk conductance of the pore with DNA in it:

$$G_{acc_{DNA}} = G_{0acc} - G_{DNA_{acc}} = G_{0acc} - \sigma \frac{\pi d_{DNA}^2}{2d_p},$$

$$G_{pore_{DNA}} = G_{0pore} - G_{DNA_{pore}} = G_{0pore} - \sigma \frac{\pi d_{DNA}^2}{4L_{eff}},$$

where  $d_{DNA} = 2.2 \text{ nm}$ . Note we have neglected DNA surface currents, as the effective charge of the DNA in high concentration LiCl buffers is small<sup>10</sup>. The conductance blockade can be then evaluated as the difference between the conductance of the bare pore and that of a pore with DNA:

$$\Delta G_{DNA} = \left( \frac{1}{G_{0poreDNA}} + \frac{2}{G_{0accDNA}} \right)^{-1} - G_{Total}$$

Using the last equation we evaluated the conductance blockades for DNA translocations through 10 nm and 16 nm nanopores and voltages ranging from 200 mV to 500 mV.

## 7. Theoretical model of a blockade current

To explain the observed difference in conductance blockades that DNA produces in individual solid-state nanopores and when trapped simultaneously by the two pores, we developed a theoretical model that is schematically illustrated in Figure S8. In this model, the space is divided into three compartments: cis, trans, and the nanopore volume. Total resistance of the system is, therefore, the sum of resistances of the compartments:  $R_{total} = R_{cis} + R_{pore} + R_{trans}$ . Ionic current that flows through the pore under an applied bias  $U$  can be readily computed as  $I = U / R_{total}$ . To estimate the three components of the total resistance, we consider neutral nanopores of a cylindrical shape. In doing so we neglect the change in ion behavior near the charged membrane surfaces.

We start by noting that resistances of cis and trans compartments in the absence of DNA can be estimated according to the classical formula for access resistance of a cylindrical pore:  $R_{acc} = (2 D \sigma_{bulk})^{-1}$ , where  $D$  is the diameter of a pore, and  $\sigma_{bulk}$  is conductivity of bulk electrolyte solution. When DNA translocates through the pore, it occludes both of these compartments (cis and trans) and changes their resistances. To estimate access resistance in the presence of DNA, we use the approach of Carlsen et al. <sup>6</sup>

$$R_{acc\ DNA} = \frac{1}{G_{acc\ DNA}} = \frac{1}{G_{acc} - \Delta G_{DNA}} = \frac{1}{\frac{1}{R_{acc}} - \sigma_{bulk} \frac{\pi d_{DNA}^2}{2D}} = \frac{1}{2D\sigma_{bulk} - \sigma_{bulk} \frac{\pi d_{DNA}^2}{2D}}$$

The open pore resistance can be computed based on the geometrical expression for the nanopore volume resistance and access resistance in the absence of DNA ( $R_{acc}$ ):<sup>11</sup>

$$R_{open\ pore} = R_{pore} + 2R_{acc} = \frac{L}{\sigma_{bulk} S} + \frac{1}{D\sigma_{bulk}} = \frac{L/S + 1/D}{\sigma_{bulk}}$$

where  $L$  and  $S$  are the pore length and cross-sectional area.

To calculate resistance of the middle compartment (nanopore) in the presence of DNA, we split the nanopore volume into thin “slabs” perpendicular to the nanopore axis, see Figure S8b. As these slabs are connected in series (see the equivalent electrical diagram in Figure S8c), the overall resistance of the nanopore volume  $R_{pore}$  is, therefore, the sum of resistances of these slabs:  $R_{pore} = \sum_i R_i$ . Resistance of an individual slab can be calculated according to the definition as:

$$R_i = \frac{\Delta l}{\langle \sigma_i \rangle s_i}$$

where  $\langle \sigma_i \rangle$  is the average conductivity, and  $\Delta l$  and  $s_i$  are the thickness along the pore axis and cross-sectional area of the slab, correspondingly, see Figure S8b. To compute the average conductivity  $\langle \sigma_i \rangle$  of a slab, we recall that local current density can be written as:

$$\vec{j} = \sum_{\substack{ion \\ types}} nq\vec{v} = \sum_{\substack{ion \\ types}} nq\mu\vec{E} = \sigma\vec{E}$$

where  $n$ ,  $q$ ,  $\vec{v}$ , and  $\mu$  are number density, charge, velocity, and mobility of ions,  $\sigma$  is local conductivity of the medium, and  $\vec{E}$  is the local electric field. From here it follows that local conductivity at the position defined by a radius vector  $\vec{r}$  can be computed as  $\sigma(\vec{r}) = \sum_{\substack{ion \\ types}} q n(\vec{r}) \mu(\vec{r})$ . Therefore, average conductivity of  $i$ -th slab can be computed as:

$$\langle \sigma_i \rangle = \frac{1}{s_i} \sum_{\substack{ion \\ types}} \int_{s_i} q n(\vec{r}) \mu(\vec{r}) dS$$

where summation is performed across all types of ions in the solution, and integration is performed across the cross-sectional area of a slab  $s_i$ . The only assumption we made while arriving at this expression was that local ion velocity is linearly proportional to the local electric field, i.e.  $\vec{v} = \mu\vec{E}$ , which should be valid for such a small species as ions. When the above expression is substituted into the expression of the resistance of a slab, cross-sectional area terms  $s_i$  cancel out and we arrive at the following expression:  $R_i = \Delta l \left( \sum_{\substack{ion \\ types}} \int_{s_i} q n(\vec{r}) \mu(\vec{r}) dS \right)^{-1}$ . Finally, the total nanopore resistance can be written as:

$$R_{total} = 2R_{acc\ DNA} + \sum_{i\ (slabs)} \Delta l \left( \sum_{\substack{ion \\ types}} \int_{s_i} q n(\vec{r}) \mu(\vec{r}) dS \right)^{-1}$$

In our model, we approximate the DNA conformation inside the pore with a straight line, Figure S8a-b. For simplicity and clearness, we use two points,  $\vec{M}$  and  $\vec{N}$ , to define the conformation of the DNA molecule. To perform numerical integration using the above equation each slab is discretized into rectangular parallelepiped bins  $(\Delta x, \Delta y, \Delta l)$  and integration  $\int_{s_i} dS$  is replaced by a double summation  $\sum_x \sum_y \Delta x \Delta y$ . Contribution of a particular bin to average conductivity of a slab is determined by the distance  $d$  from the center of the

bin,  $\vec{P}$ , to DNA, see Figure S8b. Within our model, this distance is set by a simple expression for the distance from a point to a line  $d = |(\vec{P} - \vec{N}) \times (\vec{M} - \vec{N})|$ . Distance from the DNA is then used to find number density  $n$  and mobility  $\mu$  for all types of ions in that bin using the profiles reported in <sup>12</sup>. Obtained distributions of  $\mu(\vec{r})$  and  $n(\vec{r})$  across all bins in a slab are then used to compute the integral  $\int_{s_i} q n(\vec{r}) \mu(\vec{r}) dS$  numerically as  $\sum_x \sum_y q \mu(x, y, z_i) n(x, y, z_i) dx dy$ . Resistance of a slab is then computed as:

$$R_{slab}(z = z_i) = \frac{\Delta l}{\sum_{types}^{ion} \sum_x \sum_y q \mu(x, y, z_i) n(x, y, z_i) \Delta x \Delta y}$$

The final expression for the total resistance of a nanopore with DNA can be written as:

$$\begin{aligned} R_{total} &= 2R_{acc\ DNA} + \sum_{slabs(z_i)} \frac{\Delta l}{\sum_{types}^{ion} \sum_x \sum_y q \mu(x, y, z_i) n(x, y, z_i) \Delta x \Delta y} = \\ &= \frac{1}{D\sigma_{bulk} - \sigma_{bulk} \frac{\pi d_{DNA}^2}{4D}} + \sum_{slabs(z_i)} \frac{\Delta l}{\sum_{types}^{ion} \sum_x \sum_y q \mu(x, y, z_i) n(x, y, z_i) \Delta x \Delta y} \end{aligned}$$

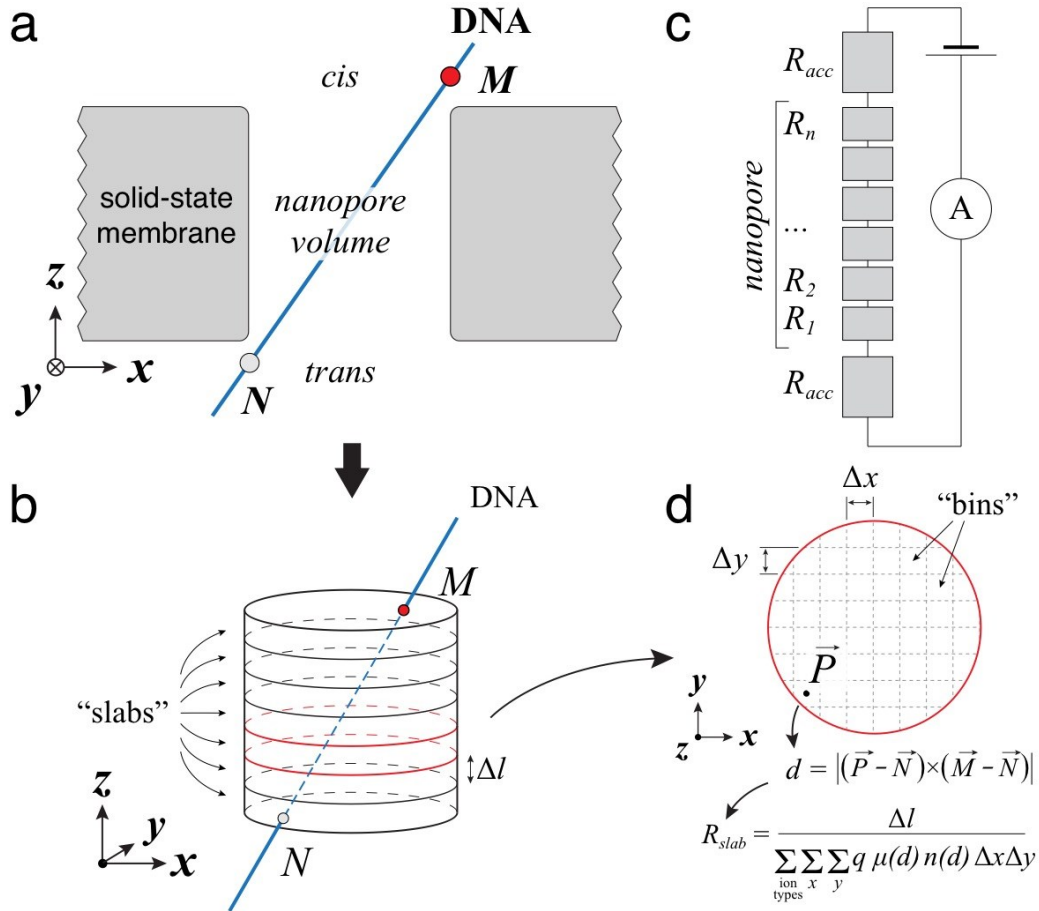


Figure S8. Theoretical model of the nanopore resistance. (a) Schematic representation of the overall model. The DNA molecule is shown as a blue line, solid-state membrane – as a gray surface. Points  $M$  and  $N$  define the orientation of DNA with respect to the nanopore. (b) Schematic representation of the nanopore volume containing a straight DNA molecule. The nanopore volume is split into horizontal slabs that are perpendicular to the nanopore axis ( $z$ ). Each slab has the same height  $\Delta l$  along the  $z$  axis. (c) An equivalent electrical diagram of the employed theoretical model. (d) Top view of a slab and its discretization into bins. Shortest distance from the center of a bin (point  $\vec{P}$ ) to DNA is computed as  $d = |(\vec{P} - \vec{N}) \times (\vec{M} - \vec{N})|$ . This distance is then used to determine mobility and number density of ions in that bin, which are then used to compute average conductivity of the slab. Resistance  $R_{slab}$  of a slab is calculated as an inverse average conductivity of a slab  $\sigma$  scaled by ratio of the slab's thickness  $\Delta l$  and its cross-sectional area  $S$ .

## 7.1 Verification of the theoretical model

We verified our theoretical model for two simple scenarios. First, we considered the case when no DNA was present in the nanopore, so that conductivity and mobility in each bin of every slab was equal to those of the bulk solution. The calculated resistance of the nanopore volume was found to closely follow the classical geometry-based expression  $R = \frac{\Delta l}{\sigma S}$ . Then, we considered the case of DNA is placed in the pore center along the nanopore axis and computed the changes in the conductance, resistance, and ionic current for various diameters of the pore, Figure S9a-c. As it follows from the figure, DNA changes the conductance of a nanopore volume by the same amount if the nanopore radius exceeds 25 Å, see Figure S9a, blue circles. At the same time, the effect of DNA on the conductance of access regions depends on the pore radius, which results in the overall non-trivial dependence of conductance blockade on the pore diameter. The change in the resistance of a nanopore due to the presence of the molecule depends on the radius of the nanopore, Figure S9b. For example, the molecule increases the resistance by 0.718 Mohm in a 10 nm pore, but only by 0.167 Mohm in the 15 nm pore. As it follows from Figure S9a, the model predicts conductance blockades of 3.26 nS and 2.48 nS for 10 and 15 nm nanopores, correspondingly. These values are in excellent quantitative agreement with experimentally obtained values of 3.35 nS and 2.50 nS.

## 7.2 Calculation of the conductance blockade for obliquely oriented DNA in a nanopore

Using the described model for the nanopore resistance, we computed 2-D current blockade maps shown in Figure S10(d-e). For this purpose, we performed a series of calculations in which we varied the position of the point  $N$ , while keeping position of the point  $M$  fixed. Point  $M$  was positioned in such a way that DNA was touching the corner of the cylindrical nanopore. Such a position of point  $M$  corresponds to the case when DNA is trapped by both pores in the double-nanopore system and is stretched between them. For each position of  $N$  we computed the nanopore resistance using the above expression and Li and Cl ion mobility and number density profiles reported in Figures S3 and S6, respectively, of Ref. <sup>12</sup>. Bulk conductivity of the solution was calculated as  $\sigma_{bulk} = q_{Li}\mu_{Li,bulk}n_{Li,bulk} + q_{Cl}\mu_{Cl,bulk}n_{Cl,bulk} = 18.2$  S/m, and DNA diameter  $d_{DNA}$  was set to 2.2 nm. Following that we computed the open pore resistance,  $R_{open\ pore}$ . To directly compare the results of our calculations to experiment, all resistance values were scaled by the ratio of bulk electrolyte conductivities in simulations and experiment, *i.e.*:  $\frac{\sigma_{bulk}}{\sigma_{exp}}$ , where  $\sigma_{exp}$  is the experimental value

of solution conductivity equal to 13.2 S/m. Using the obtained resistance values, we computed the resistance increase,  $\Delta R = R_{total} - R_{open\ pore}$ , and the conductance blockade,  $\Delta G = \frac{1}{R_{total}} - \frac{1}{R_{open\ pore}}$ . Corresponding current blockade  $\Delta I$  was then calculated as a product of the conductance blockade  $\Delta G$  and the applied bias voltage  $V$ .

Using the obtained maps, Figure S9d and e, we compute the limits on the ionic current blockade reported in Main Text Figure 6c. As expected, the highest current blockade corresponds to the scenario when DNA spans across the pore in an oblique orientation, while the lowest current blockades corresponds to the scenario in which DNA is oriented parallel to the nanopore axis and located near the nanopore wall ('hugging the nanopore').

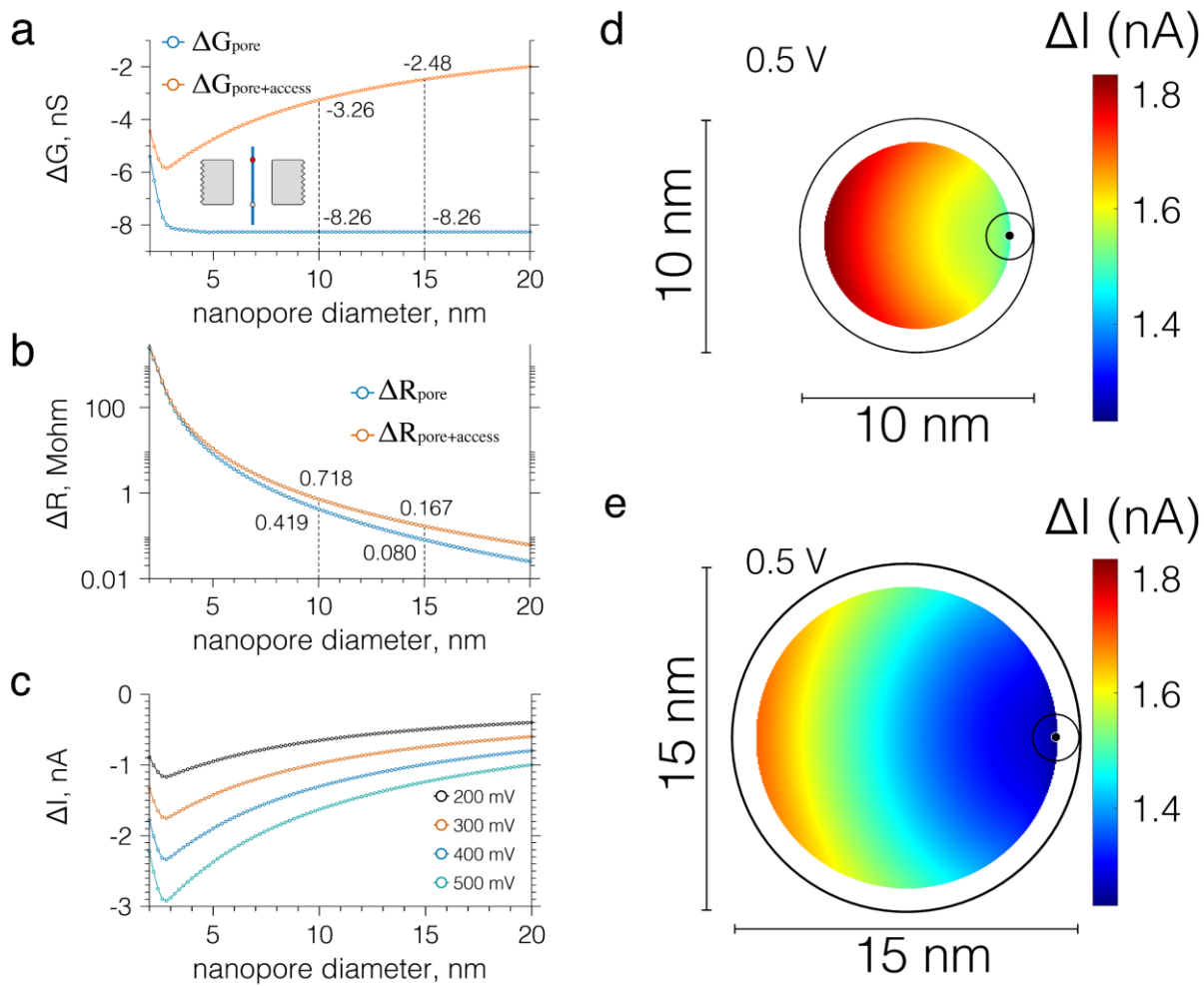


Figure S9. Nanopore blockade currents according to the theoretical model. Changes in nanopore conductance (a), resistance (b), and ionic current (c) as a function of the nanopore radius produced by a DNA molecule positioned in the middle of the nanopore and parallel to its axis. Panels a and b also show corresponding changes for conductance and resistance of the nanopore volume only (blue circles). Vertical dashed lines indicate the values obtained for the nanopores 10 and 15 nm in diameter. For pores larger than 5 nm in diameter, DNA decreases conductance of the nanopore volume by the same amount. At the same time, the increase of the nanopore resistance caused by the presence of DNA depends on the pore radius. (d-e) Example of the 2-D maps of ionic current blockades. Point *M* (defined in Figure S8) is shown as a black dot with a circle around it; the circle indicates the cross-section of DNA. The highest current blockade is achieved when DNA spans across the pore, whereas the lowest one corresponds to DNA positioned near the nanopore surface and oriented parallel to its axis.

## 8. Criteria for determining escape direction in a double-nanopore event

Using Figure S7 we determined  $\Delta I_{10}$  or  $\Delta I_{16}$ , which are current blockades produced by single linear dsDNA molecule translocating through either 10 or 16 nm pores, respectively. The observed blockade levels at the end signature (the region of the current trace where DNA escapes the double-nanopore event and thus resides only in one of the nanopores) was without exception, close to but slightly larger than the blockade levels observed from single-pore translocations. We suggest that this is caused by the DNA still being partly in the tilted orientation (see Section 7 of this document) after exiting the first pore, thus producing a larger blockade (cf previous section). Hence, we used the following criteria to assign the escape direction. If the blockade level of the end signature was between  $\Delta I_{16}$  and  $\Delta I_{10}$ , the DNA final exit was ascribed to the 16 nm pore. For all end signature blockade levels larger than  $\Delta I_{10}$ , DNA exit was ascribed to the 10 nm pore. No blockades smaller than  $\Delta I_{16}$  were observed in the experiment.

**9. Additional set of experiments characterizing the entrance and exit of DNA from an asymmetric double-nanopore system.**

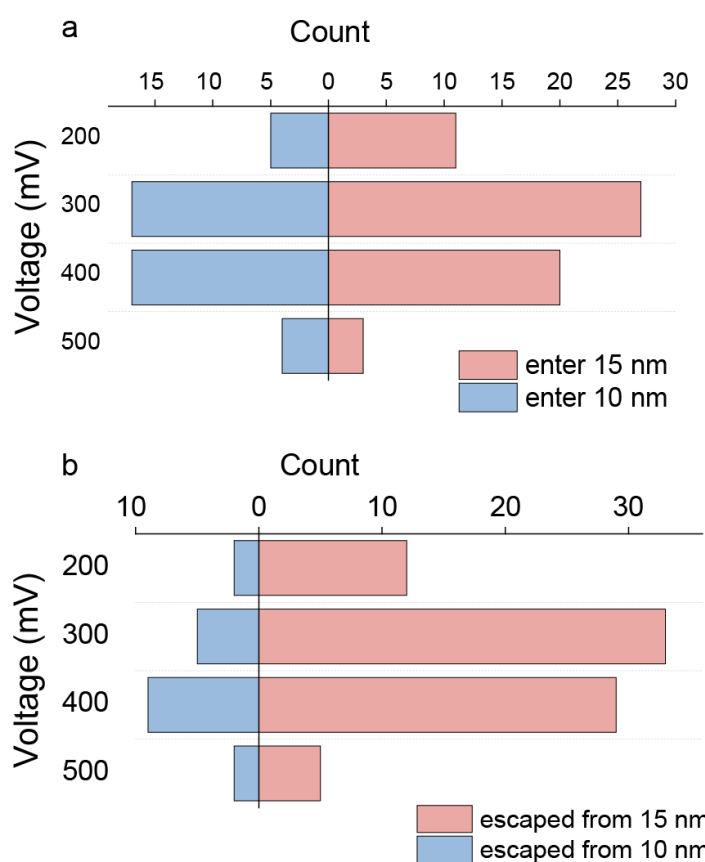


Figure S10 The number of double-nanopore events that (a) started with DNA entering the 15 nm pore (red) or the 10 nm pore (blue); (b) ended with DNA escaping the 15 nm pore (red) or the 10 nm pore (blue). This set of experiment was performed using a system of two pores, 10 and 15 nm in diameter, separated by 300 nm. The data are in agreement with the behaviour observed for the 10 nm / 16 nm asymmetric double-nanopore system characterized in Figure 6 of the Main Text.

**10. Equivalent circuit for the asymmetric double-nanopore system.**

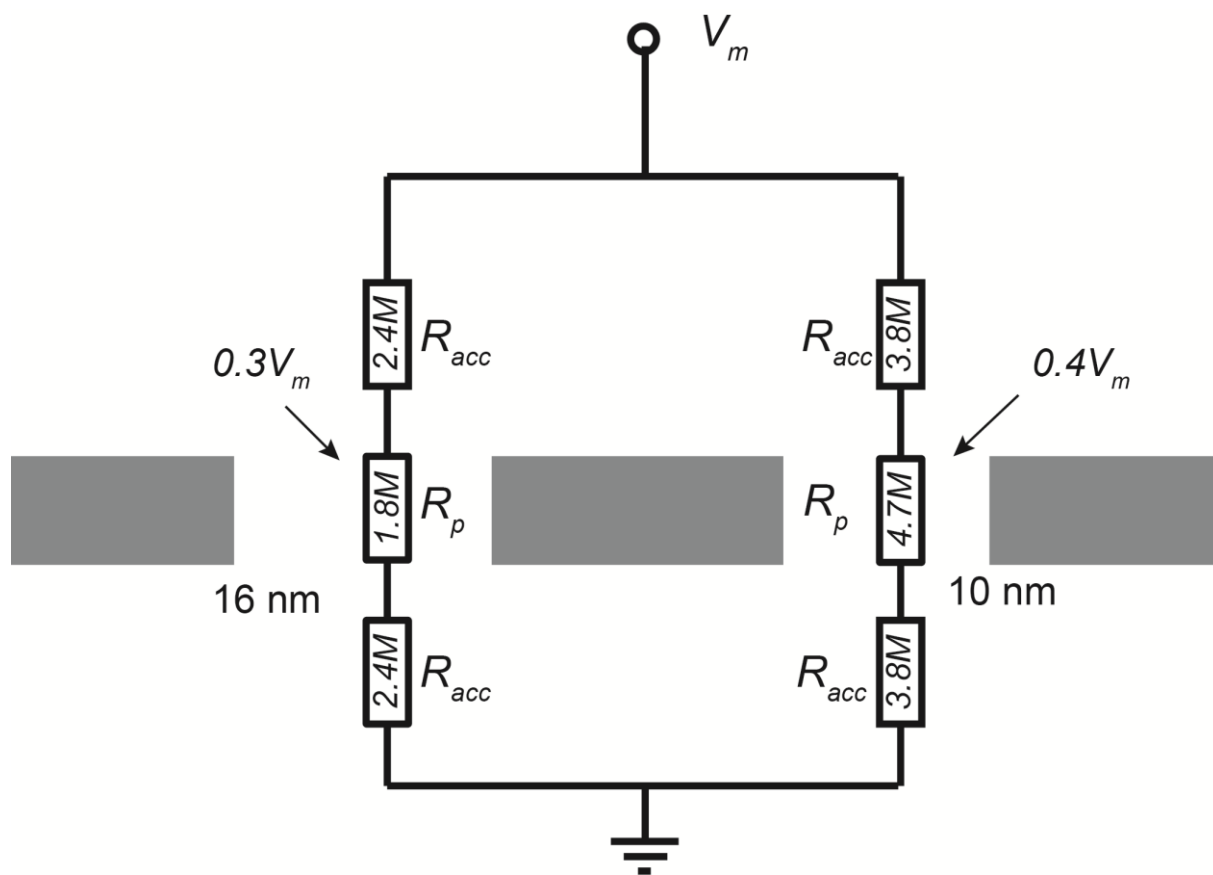


Figure S11. Equivalent circuit of the asymmetric double-nanopore system. The resistances were calculated based on the model described in Section S6 of Supporting Information.

## 11. Calculation of the forces acting on the DNA in the access region

The force of the transmembrane bias exerted on DNA in the access resistance region was estimated using the electrostatic model (Figure S12) built on the following assumptions:

1. The electric field near a nanopore can be approximated by the potential of a point-like charge<sup>13</sup>:

$$V(r) = \frac{d^2}{8lr} V_m$$

$$E(r) = -\frac{dV}{dr} = \frac{d^2}{8lr^2} V_m$$

where  $d$  is the pore diameter,  $l$  is the effective pore length,  $r$  is the distance from the pore and  $V_m$  is the transmembrane voltage

2. DNA is treated as a charged rod with the surface charge density<sup>14</sup>  $\sigma = 10.5 \text{ mC/m}^2$ , allowing for an increased effective screening<sup>10</sup>. This corresponds to a linear charge density  $\lambda = 2\pi r_{DNA}\sigma$  of  $0.073 \times 10^{-9} \text{ C/m}$ .
3. DNA is stretched along the  $x$  axis (see Fig. S13). The charge of a DNA fragment of length  $dx$  thus equals to  $dq = \lambda dx$

The force acting on each infinitesimal partition of DNA can thus be evaluated as:

$$dF = dq \times E = \frac{d^2}{8lx^2} \lambda dx$$

$$F = \int_{x_1}^{x_D} dF = \frac{d^2 \lambda}{8l} \left( \frac{1}{x_1} - \frac{1}{x_D} \right)$$

where  $x_D$  is the distance between two pores, and  $x_1$  is the coordinate of the nanopore wall. This leads to the result displayed in Figure S13, which shows the forces exerted on DNA as a function of nanopore distance (Figure S13a) and voltage (Figure S13b) by each of the pores and the difference of the two forces. The essential point is that the force pulling the DNA toward the 16 nm pore is much larger (by 3-8 pN) than the force pulling the DNA toward the 10 nm pore. The difference of the two forces explains the preference for the DNA to exit through the 16 nm-diameter pore.

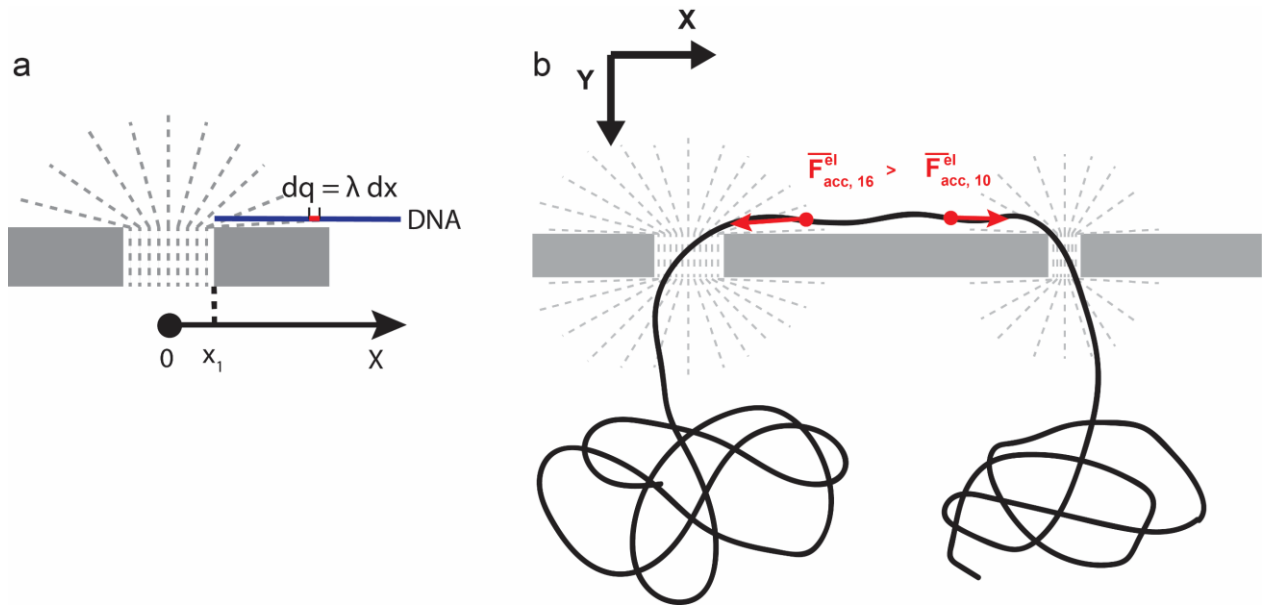


Figure S12. (a) Sketch of the model used for the calculation of the electric forces exerted on DNA by the transmembrane bias in the access region. The DNA molecule is shown as a blue line; the electric field lines as grey dashed lines. (b) Sketch of the forces exerted by access regions on DNA

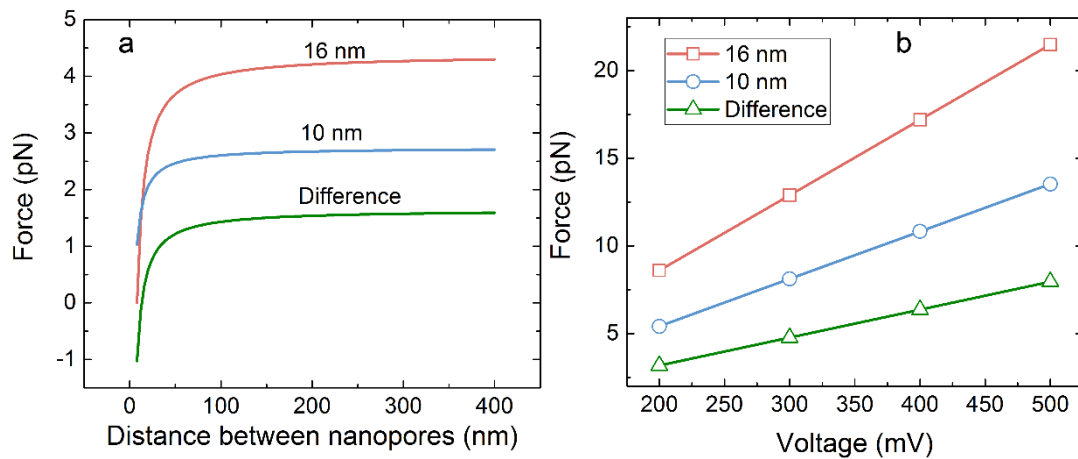


Figure S13. Force exerted on DNA by the electric field in the access region, (a) plotted as a function of distance between nanopores (at  $V_m = 100$  mV) and (b) as a function of transmembrane voltage (at 400 nm distance between the nanopores).

## 12. Movies generated by MD simulations

Movie1. Single-pore translocation event featured in the top panel of Figure 4b. The pore separation was 750 nm. The applied bias was 125 mV. The P and B beads of DNA are shown as orange and pink spheres, respectively.

Movie2. Double-nanopore translocation event featured in the bottom panel of Figure 4b. The pore separation was 750 nm. The applied bias was 125 mV. The P and B beads of DNA are shown as orange and pink spheres, respectively. The DNA was captured by simultaneously by two pore during the translocation process.

Movie3. Ensemble of DNA conformations observed during DNA translocation simulations. Shown in grey are the 2000 instantaneous conformations of DNA overlaid with each other. The DNA molecules simultaneously captured by the two pores are highlighted using a darker shade of grey. The color contours specify the density of the CG beads computed from the position of beads projected onto the XZ plane, over a  $1 \text{ nm}^2$  grid.

## References

1. Phillips, J. C. *et al.* Scalable molecular dynamics with NAMD. *J. Comput. Chem.* **26**, 1781–1802 (2005).
2. Maffeo, C., Ngo, T. T. M., Ha, T. & Aksimentiev, A. A coarse-grained model of unstretched single-stranded DNA derived from atomistic simulation and single-molecule experiment. *J. Chem. Theory Comput.* **10**, 2891–2896 (2014).
3. Nkodo, A. E. *et al.* Diffusion coefficient of DNA molecules during free solution electrophoresis. *Electrophoresis* **22**, 2424–2432 (2001).
4. Belkin, M., Chao, S. H., Jonsson, M. P., Dekker, C. & Aksimentiev, A. Plasmonic Nanopores for Trapping, Controlling Displacement, and Sequencing of DNA. *ACS Nano* **9**, 10598–10611 (2015).
5. Wells, D. B., Abramkina, V. & Aksimentiev, A. Exploring transmembrane transport through alpha-hemolysin with grid-steered molecular dynamics. *J. Chem. Phys.* **127**, (2007).
6. Carlsen, A. T., Zahid, O. K., Ruzicka, J., Taylor, E. W. & Hall, A. R. Interpreting the conductance blockades of DNA translocations through solid-state nanopores. *ACS Nano* **8**, 4754–4760 (2014).
7. Wanunu, M. *et al.* Rapid electronic detection of probe-specific microRNAs using thin nanopore sensors. *Nat. Nanotechnol.* **5**, 807–14 (2010).
8. Kowalczyk, S. W., Grosberg, A. Y., Rabin, Y. & Dekker, C. Modeling the conductance and DNA blockade of solid-state nanopores. *Nanotechnology* **22**, 315101 (2011).
9. Nicoli, F., Verschueren, D., Klein, M., Dekker, C. & Jonsson, M. P. DNA translocations through solid-state plasmonic nanopores. *Nano Lett.* **14**, 6917–25 (2014).
10. Kowalczyk, S. W., Wells, D. B., Aksimentiev, A. & Dekker, C. Slowing down DNA Translocation through a Nanopore in Lithium Chloride. *Nano Lett.* **12**, 1038–1044

- (2012).
11. Hall, J. E. Access Resistance of a Small Circular Pore. *J. Gen. Physiol.* **66**, 531–532 (1975).
  12. Belkin, M. & Aksimentiev, A. Molecular Dynamics Simulation of DNA Capture and Transport in Heated Nanopores. *ACS Appl. Mater. Interfaces* **8**, 12599–12608 (2016).
  13. Grosberg, A. Y. & Rabin, Y. DNA capture into a nanopore: Interplay of diffusion and electrohydrodynamics. *J. Chem. Phys.* **133**, (2010).
  14. Chen, L. & Conlisk, A. T. Forces affecting double-stranded DNA translocation through synthetic nanopores. *Biomed. Microdevices* **13**, 403–414 (2011).